Modeling and predicting rogue waves in deep water

C. M. Schober

University of Central Florida, Orlando, Florida - USA

Abstract. We investigate rogue waves in the framework of the nonlinear Schrödinger (NLS) equation and correlate the development of rogue waves in oceanic sea states characterized by the JONSWAP spectrum with the proximity to homoclinic solutions of the NLS equation. Using the inverse spectral theory of the NLS equation, we introduce the "splitting distance" δ between two simple points in the discrete Floquet spectrum of the associated AKNS problem, as a way of determining the proximity in spectral space to instabilities and homoclinic data of the NLS equation (*Islas and Schober*, 2005). In several hundred simulations of the NLS equation, where the parameters and the phases in the JONSWAP initial data are varied, we find that (i) rogue waves develop whenever the splitting distance δ is small and (ii) rogue waves do not occur when the splitting distance δ is large.

Introduction

In the past several years there has been particular interest in understanding the physical processes responsible for the generation of rogue waves. According to Rayleigh's distribution of wave heights, an extremely unlikely wave event, a rogue wave, is a high amplitude wave whose height exceeds 2.2 times the significant wave height H_s of the background sea (*Kharif and Pelinovsky*, 2003). Rogue waves have been observed in both shallow and deep water, with or without the presence of strong currents. Several mechanisms have been proposed to explain their formation subject to the specific physical conditions (e.g., *Olagnon and Athanassoulis* 2000; *Henderson et al.*, 1999; *Trulsen and Dysthe*, 1997; *Pelinovsky et al.*, 2001; *Brown*, 2001).

In the linear theory, the wave field is assumed to be the superposition of a large number of small amplitude, monochromatic waves, with random, uniformly distributed frequencies and phases. The occurrence of rogue waves can be due to space-time caustics, dispersion phenomena, spatial focusing, and wave-current interactions (*Brown*, 2001; *Kharif and Pelinovsky*, 2003). However, upon analyzing satellite data the European MAXWAVE project detected more extreme waves than predicted by the standard linear theory (*Lehner et al.*, 2004).

One of the proposed mechanisms for the generation of rogue waves in the open ocean is nonlinear self focusing due to effects like the Benjamin Feir (BF) instability (e.g., *Henderson et al.*, 1999; *Calini and Schober*, 2002; *Kharif et al.*, 2001; *Onorato et al.*, 2001a; and *Pelinovsky et al.*, 2000). The BF instability, where a uniform train of surface waves is unstable to a weak amplitude modulation, is described to leading order by the focusing nonlinear Schrödinger (NLS) equation

$$iu_t + u_{xx} + 2|u|^2 u = 0. \tag{1}$$

The NLS equation has proven to be an excellent model for initiating studies of rogue waves in deep water. A linearized analysis of the NLS equation shows that low-frequency modes may become unstable and that the number of unstable modes increases with the amplitude of the carrier wave. The complete integrability of the NLS equation allows one to use Bäcklund transformations to compute homoclinic solutions (*Ercolani et al.*, 1990) and thus study the nonlinear evolution of the instabilities. In the simplest setting homoclinic orbits of the unstable Stokes solution of the NLS equation have been used for modeling rogue waves (*Osborne et al.*; 2000, *Calini and Schober*, 2002). Homoclinic solutions of the NLS equation with a complex space-time structure, obtained with two or more unstable modes, can be phase modulated so that the modes are excited simultaneously (optimal phase modulation), or nearly so. In this case, the wave amplification is due to both the BF instability and the additional phase modulation (see Fig. 1a) (*Calini and Schober*, 2002).

The NLS equation is the leading order equation in a hierarchy of envelope equations and is derived from the full water wave equations under the assumption of a narrow $\mathcal{O}(\epsilon)$ banded spectrum. This bandwidth constraint limits the applicability of the NLS equation in 2D as it results in energy leakage to high wave number modes. A more accurate description of water wave dynamics is provided by, for example, the fourth-order modified Dysthe (MD) equation, derived by assuming the bandwidth is $\mathcal{O}(\sqrt{\epsilon})$ and by retaining higher order terms in the asymptotic expansion for the surface wave displacement (*Trulsen and Dysthe*, 1996). The MD equation is able to capture higher-order physical ef-

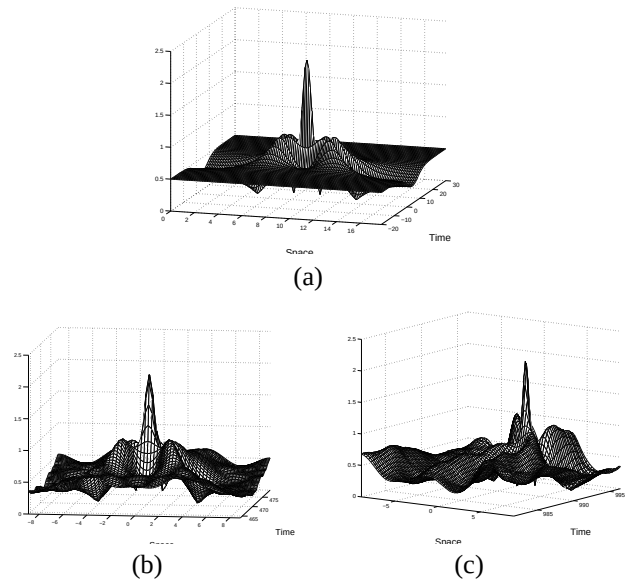

(a) (b) (c)

Figure 1. Wave amplification due to amplitude and phase modulation for the (a) NLS equation, and for the MD equation in the even (b) and noneven (c) regimes.

fects such as asymmetric evolution of wave packets and side bands and also limits the energy leakage to higher modes that are obtained in 2D with the NLS equation (*Trulsen and Dysthe*, 1996; *Trulsen and Dysthe*, 1997).

"Noisy" rogue waves, i.e. rogue waves with a chaotic background, are observed in numerical simulations of both the full MD equation,

$$iu_t + u_{xx} + 2|u|^2u = \epsilon\left(-\tfrac{i}{2}u_{xxx} + 6i|u|^2u_x \right. \\ \left. -iu^2u_x^* - 8u\bar{\phi}_x + \tfrac{5}{16}u_{xxxx} + \tfrac{7i}{32}u_{xxxxx}\right), \quad (2)$$

and under the restriction to spatially symmetric wave trains. In a chaotic regime of homoclinic type, the solution can evolve close to an optimal phase modulated homoclinic solution for a rather general class of initial conditions, even when the initial data have not been selected to generate a phase modulation (Fig. 1b-c). The chaotic dynamics due to BF instability and higher order nonlinear effects allow for enhanced focusing to occur due to chaotically generated optimal phase modulations (*Calini and Schober*, 2002).

Viewing the MD equation as a perturbation of the NLS equation, a Mel'nikov analysis shows that homoclinic orbits of the Stokes wave persist for the MD equation in the even regime (*Calini and Schober*, 2002). Significantly, the Melnikov analysis also predicts the same distinguishing spatial features of the perturbed dynamics as those observed in the numerical experiments. The homoclinic orbit (or rogue wave) selected by the Melnikov analysis is $\mathcal{O}(\epsilon)$ close to the optimal phase modulated NLS homoclinic solution (Fig. 1a) and is observed in the numerical simulations (Fig. 1b).

This persistence result places the notion that homoclinic solutions of the NLS equation are significant in modeling rogue waves on a firmer mathematical footing and led us to conjecture that one approach to predicting rogue waves in realistic oceanic states would be to determine the proximity of a sea state to homoclinic data of the NLS equation.

Developing sea states are described by the Joint North Sea Wave Project (JONSWAP) power spectrum (e.g., *Ochi*, 1998). In numerical simulations of the NLS equation (*Onorato et al.*, 2001a) examined the generation of extreme waves for typical random oceanic sea states characterized by the JONSWAP power spectrum. It was found that rogue waves occur more often for large values of the Phillips parameter α and the enhancement coefficient γ in the JONSWAP spectrum. Even so, they observed that large values of α and γ do not guarantee the development of extreme waves.

Two of our results that we want to emphasize in this paper are (i) the dependence of rogue wave events on the phases in the "random phase" reconstruction of the surface elevation (see eqn. (5)) and (ii) the usefulness of the nonlinear spectral decomposition in providing a simple criterium, in terms of the proximity to homoclinic solutions, for predicting the occurrence and strength of rogue waves (see *Islas and Schober*, 2005). We find that the phase information is as important as the amplitude and peakedness of the wave (governed by α and γ) when determining the occurrence of rogue waves. Random oceanic sea states characterized by JONSWAP data are not small perturbations of Stokes wave solutions. As a consequence, it is difficult to investigate the generation of rogue waves in more realistic sea states using a linear stability analysis (as in the Benjamin-Feir instability). Our approach uses the inverse spectral theory of the NLS equation to examine a nonlinear mode decomposition of JONSWAP type initial data. We introduce a spectral quantity, the "splitting distance" δ between two simple points in the discrete Floquet spectrum of the associated AKNS problem, as a way of determining the proximity in spectral space to instabilities and homoclinic solutions of the NLS equation.

Our main results are these: (1) JONSWAP data can be quite near data for homoclinic orbits of complicated N-phase solutions. For fixed values of α and γ in the JONSWAP spectrum, as the phases in the initial data are randomly varied, the proximity δ to homoclinic data varies. (2) In several hundred simulations of the NLS equation, where the parameters and the phases in the JONSWAP initial data are varied, we find that (i) rogue waves develop whenever the splitting distance δ is small and (ii) rogue waves do not occur when the splitting distance δ is large (*Islas and Schober*, 2005). This is the first time that this quantitative approach has been used in processing water wave data and that homoclinic solutions have been correlated with rogue waves for random sea states.

JONSWAP initial data

To examine the generation of rogue waves in a random sea state, we consider initial free surface elevation data of the form

$$\eta(x,0) = \sum_{n=1}^{N} C_n \cos(k_n x - \phi_n),$$

where C_n is the amplitude of the nth component with wave number $k_n = (n-1)k$, $k = 2\pi/L$, and random phase ϕ_n, uniformly distributed on the interval $(0, 2\pi)$. The spectral amplitudes, $C_n = \sqrt{2S_n/L}$, are obtained from the JONSWAP spectrum (*Onorato et al.*, 2001b):

$$S(f) = \frac{\alpha}{f^5}\exp\left[-\frac{5}{4}\left(\frac{f_0}{f}\right)^4\right]\gamma^r, \quad (3)$$

$$r = \exp\left[-\frac{1}{2}\left(\frac{f-f_0}{\sigma_0 f_0}\right)^2\right]. \quad (4)$$

Here f_0 is the dominant frequency, determined by the wind speed at a specified height above the sea surface, and $\sigma_0 = 0.07\ (0.9)$ for $f \le f_0$ $(f > f_0)$. As the parameter γ is increased, the spectrum becomes narrower about the dominant peak. The parameter α is related to the amplitude and energy content of the wavefield. Based on an "Ursell number", the ratio of the nonlinear and dispersive terms of the NLS equation (1) in dimensional form, the NLS equation is considered to be applicable for $2 < \gamma < 8$ and $0.008 < \alpha < 0.02$ (*Onorato et al.*, 2001a).

The surface elevation η is related to u, the solution of the NLS equation, by $\eta = \mathrm{Re}\left\{iue^{ikx}\right\}/\sqrt{2}k$. Using the Hilbert transform of η and its associated analytical signal, the initial condition for u can be modeled as the random wave process

$$u(x,0) = -i\sum_{n=1}^{N} C_n \exp\left[i\left(k_{n-1}x - \phi_n\right)\right]. \quad (5)$$

We examine a nonlinear spectral decomposition of the JONSWAP initial data, which takes into account the phase information ϕ_n. This decomposition is based upon the inverse scattering theory of the NLS equation, a procedure for solving the initial value problem analogous to Fourier methods for linear problems. We find that we are able to predict the occurrence of rogue waves in terms of the proximity δ to distinguished points of the discrete spectrum. We briefly recall elements of the nonlinear spectral theory of the NLS equation.

Floquet spectral theory

The integrability of the NLS equation (1) is related to the following pair of linear systems (the so-called Lax pair)

$$\mathcal{L}^{(x)}\phi = \begin{pmatrix} D_+ & -u \\ u^* & D_- \end{pmatrix}\begin{pmatrix} \phi_1 \\ \phi_2 \end{pmatrix} = 0, \quad \mathcal{L}^{(t)}\phi = 0, \quad (6)$$

where $D_\pm = \partial/\partial x \pm i\lambda$, λ is the spectral parameter and ϕ is the eigenfunction (*Ablowitz and Segur*, 1981). These systems have a common nontrivial solution $\phi(x,t;\lambda)$, provided the potential $u(x,t)$ satisfies the NLS equation. $\mathcal{L}^{(t)}$ is not specified explicitly as it is not implemented in our analysis.

The first step in solving the NLS using the inverse scattering theory is to determine the spectrum

$$\sigma(u) = \left\{\lambda \in \mathbb{C} \mid \mathcal{L}^{(x)}\phi = 0, |\phi| \text{ bounded } \forall x\right\}$$

of the associated linear operator $\mathcal{L}^{(x)}$, which is analogous to calculating the Fourier coefficients in Fourier theory. For periodic boundary conditions, $u(x+L,t) = u(x,t)$, the spectrum of u is expressed in terms of the transfer matrix $M(x+L;u,\lambda)$ across a period, where $M(x;u,\lambda)$ is a fundamental solution matrix of the Lax pair (6). Introducing the Floquet discriminant $\Delta(u,\lambda) = \mathrm{Trace}\left[M(x+L;u,\lambda)\right]$, one obtains (*Ablowitz and Segur*, 1981)

$$\sigma(u) = \left\{\lambda \in \mathbb{C} \mid \Delta(u,\lambda) \in \mathbb{R},\ |\Delta(u,\lambda)| \le 2\right\}. \quad (7)$$

The distinguished points of the periodic/antiperiodic spectrum, where $\Delta(\lambda,u) = \pm 2$, are

(a) simple points $\{\lambda_j^s \mid d\Delta/d\lambda \neq 0\}$ and

(b) double points $\{\lambda_j^d \mid d\Delta/d\lambda = 0,\ d^2\Delta/d\lambda^2 \neq 0\}$.

The Floquet discriminant functional $\Delta(u,\lambda)$ is invariant under the NLS flow and encodes the infinite family of constants of motion of the NLS (parametrized by the λ_j^s).

The Floquet spectrum (7) of a generic NLS potential consists of the entire real axis plus additional curves (called bands) of continuous spectrum which terminate at the simple points λ_j^s. N-phase solutions are those with a finite number of bands of continuous spectrum. Double points arise when two simple points have coalesced and their location is important.

Using the direct spectral transform, any initial condition or solution of the NLS can be represented in terms of a set of nonlinear modes. The spatial structure and dynamical stability of these modes is determined by the order and location of the corresponding λ_j as follows (*Ercolani et al.*, 1990): (a) Simple points correspond to stable active degrees of freedom. (b) Double points label all additional potentially active degrees of freedom. Real double points correspond to stable inactive (zero amplitude) modes. Complex double points are associated with all the unstable active modes and label the corresponding homoclinic orbits.

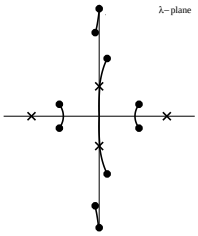

Figure 2. Spectrum of an unstable N-phase solution.

Formulas for the N-phase solutions, $\Theta(\theta_1, ..., \theta_N)$, are obtained explicitly in terms of the simple spectrum. The phases evolve according to $\theta_j = \kappa_j x + \Omega_j t + \theta_j^0$, $\kappa_j = 2\pi n_j / L$, where κ_j and Ω_j are determined by λ_j^s (since the spectrum is invariant κ_j and Ω_j are constants). For a given N-phase solution, the isospectral set (all NLS solutions with the same spectrum) comprises an N-dimensional torus characterized by the phases θ_j. If the spectrum contains complex double points, then the N-phase solution may be unstable. The instabilities correspond to orbits homoclinic to the N-phase torus.

Figure 2 shows the spectrum of a typical unstable N-phase solution. There are N bands of spectrum determined by the $2N$ simple points λ_j^s. The $2M$ complex double points λ_j^d indicate that the solution is unstable and that there is a homoclinic orbit. The simple periodic eigenvalues are labeled by circles and the double points are labeled by crosses. Under perturbations complex double points typically split into two simple points, $\lambda_\pm$, thus opening a gap in the band of spectrum. An example of spectrum for a nearby semi-stable N-phase solution where the complex double point is split $\mathcal{O}(\epsilon)$ is given in Fig. 3(a).

We denote the distance between these two simple points by $\delta(\lambda_+, \lambda_-) = |\lambda_+ - \lambda_-|$ and refer to it as the splitting distance. We use δ to measure the proximity in the spectral plane to homoclinic data, i.e. to complex double points and their corresponding instabilities. Since the NLS spectrum is symmetric with respect to the real axis and real double points correspond to inactive modes, in subsequent plots only the spectrum in the upper half complex λ-plane will be displayed.

Criterium for predicting rogue waves: proximity to homoclinic data

In the numerical simulations the NLS equation is integrated using a pseudo-spectral scheme with 256 Fourier modes in space and a fourth order Runge-Kutta discretization in time ($\Delta t = 10^{-3}$). The nonlinear mode content of the data is numerically computed using the direct spectral transform described above, i.e. the system of ODEs (6) is numerically solved to obtain the discriminant Δ. The zeros

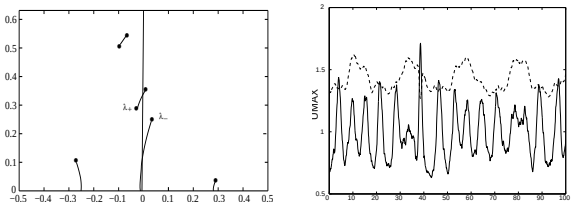

Figure 3. (a) Nonlinear spectrum and (b) evolution of U_{max} for JONSWAP data ($\gamma = 4$ and $\alpha = 0.016$) that is near homoclinic data. Dashed curve corresponds to $2.2\,H_s$.

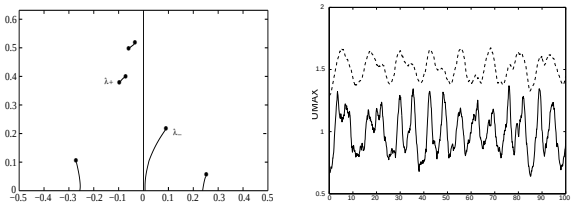

Figure 4. (a) Nonlinear spectrum and (b) evolution of U_{max} for JONSWAP data ($\gamma = 4$ and $\alpha = 0.016$) that is far from homoclinic data. Dashed curve corresponds to $2.2\,H_s$.

of $\Delta \pm 2$ are then determined with a root solver based on Muller's method (*Ercolani et al.*, 1990). The spectrum is computed with an accuracy of $\mathcal{O}(10^{-6})$, whereas the spectral quantities we are interested in range from $\mathcal{O}(10^{-2})$ to $\mathcal{O}(10^{-1})$.

We begin by determining the spectrum of JONSWAP initial data given by (5) for various combinations of $\alpha = 0.008$, 0.012, 0.016, 0.02, and $\gamma = 1, 2, 4, 6, 8$. For each such pair (γ, α), we performed fifty simulations, each with a different set of randomly generated phases. As expected, the basic spectral configuration and the number of excited modes depended on the energy and the enhancement coefficient α and γ. However, the extent of the dependence of the spectrum upon the phases in the initial data was surprising.

As a typical example of the results, Figs. 2(a) and 3(a) show the numerically computed nonlinear spectrum of JONSWAP initial data when $\gamma = 4$ and $\alpha = 0.016$ for two different realizations of the random phases. We find that JONSWAP data correspond to "semi-stable" N-phase solutions, i.e. we interpret the data as perturbations of N-phase solutions with one or more unstable modes (compare Fig. 2(a) with the spectrum of an unstable N-phase solution in Fig. 1). In Fig. 2(a) the splitting distance $\delta(\lambda_+, \lambda_-) \approx 0.07$, while in Fig. 3(a) $\delta(\lambda_+, \lambda_-) \approx 0.2$. Thus the JONSWAP data can be quite "near" homoclinic data as in Fig. 2(a) or "far" from homoclinic data as in Fig. 3(a), depending on the values of the phases ϕ_n in the initial data. For all the examined values of α and γ we find that, when α and γ are fixed, as the phases in the JONSWAP data vary, the spectral distance δ of typical JONSWAP data from homoclinic data

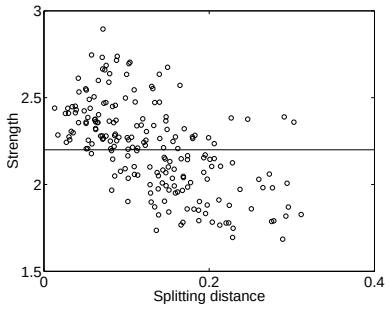

Figure 5. Strength of U_{max}/H_s vs. the splitting distance $\delta(\lambda_+, \lambda_-)$.

varies.

Most importantly, irrespective of the values of the JONSWAP parameters α and γ, in simulations of the NLS equation (1) we find that extreme waves develop for JONSWAP initial data that is "near" NLS homoclinic data, whereas the JONSWAP data that is "far" from NLS homoclinic data typically does not generate extreme waves. Figures 2(b) and 3(b) show the corresponding evolution of the maximum surface elevation, U_{max}, obtained with the NLS equation. U_{max} is given by the solid curve and as a reference, $2.2H_S$ (the threshold for a rogue wave) is given by the dashed curve. H_S is the significant wave height and is calculated as four times the standard deviation of the wave amplitude. Figure 2(b) shows that when the nonlinear spectrum is near homoclinic data, U_{max} exceeds $2.2H_S$ (a rogue wave develops at about $t = 40$). Figure 3(b) shows that when the nonlinear spectrum is far from homoclinic data, U_{max} is significantly below $2.2H_S$ and a rogue wave does not develop. In this way, we correlate the occurrence of rogue waves characterized by JONSWAP spectrum with the proximity to homoclinic solutions of the NLS equation.

The results of hundreds of simulations of the NLS equation consistently show that proximity to homoclinic data is a crucial indicator of rogue wave events. For example, Figure 4 shows the synthesis of 200 random simulations of the NLS equation for JONSWAP initial data for different (γ, α) pairs (with $\gamma = 2, 4, 6, 8$, and $\alpha = 0.012, 0.016$). For each such pair (γ, α), we performed 25 simulations, each with a different set of randomly generated phases. Each circle represents the strength of the maximum wave (U_{max}/H_S) attained during one simulation as a function of the splitting distance $\delta(\lambda_+, \lambda_-)$. The results for the particular pair $(\gamma = 4, \alpha = 0.012)$ is represented with an asterisk. A horizontal line at $U_{max}/H_S = 2.2$ indicates the reference strength for rogue wave formation. We identify two critical values $\delta_1 = 0.08$ and $\delta_2 = 0.22$ that clearly show that (a) if $\delta < \delta_1$ (near homoclinic data) rogue waves will occur; (b) if $\delta_1 < \delta < \delta_2$, the likelihood of obtaining rogue waves decreases as δ increases and, (c) if $\delta > \delta_2$ the likelihood of a rogue wave occurring is extremely small.

This behavior is robust. As α and γ are varied, the strength of the maximum wave and the occurrence of rogue waves are well predicted by the proximity to homoclinic solutions. The individual plots of the strength vs. δ for particular pairs (γ, α) are qualitatively the same as in Figure 4 as can be seen by the highlighted case $(\gamma = 4, \alpha = 0.012)$. These results provide strong evidence of the relevance of homoclinic solutions of the NLS equation in investigating rogue wave phenomena for more realistic oceanic conditions and identifies the nonlinear spectral decomposition as a simple diagnostic tool for predicting the occurrence and strength of rogue waves. Finally we note that the nonlinear spectral analysis is not limited to JONSWAP data and can be implemented for general theoretical or field data in order to predict the occurrence and strength of rogue waves.

Acknowledgments. This work was partially supported by NSF Grant No. NSF-DMS0204714.

References

Ablowitz, M. and H. Segur, *Solitons and the Inverse Scattering Transform*, SIAM, 1981.

Brown, M., Space-time surface gravity wave caustics: structurally stable extreme wave events, *Wave Motion, Elsevier*, 117-143, 2001.

Calini, A. and C. Schober, *Phys. Lett. A, 298*, 335, 2002.

Ercolani, N., M. G. Forest, and D. W. McLaughlin. Geometry of the Modulational Instability Part III: Homoclinic Orbits for the Periodic Sine-Gordon Equation, *Physica D, 43*, 349-384, 1990.

Henderson, K.L., D.H. Peregrine, and J.W. Dold, Unsteady water wave modulations: fully nonlinear solutions and comparison with the nonlinear Schrödinger equation, *Wave Motion, 29*, 341, 1999.

Islas, A., and C. Schober, Predicting rogue waves in random oceanic sea states, *Phys. Fluids, 17*, 2005.

Kharif, C., E. Pelinovsky, T. Talipova, and A. Slunyaev, Focusing of nonlinear wave groups in deep water, *Sov. Phys. JETP, 73*, 170-173, 2001.

Kharif, C. and E. Pelinovsky, Physical mechanisms of the rogue wave phenomenon, *Europ. J. Mech. B-Fluid, 22*, 603-634, 2003.

Lehner, S., H. Günther, and W. Rosenthal, Extreme wave statistics from radar data sets, *Proceedings of the IGARSS*, 2004.

Ochi, M. K., Ocean Waves: The Stochastic Approach, *Cambridge University Press*, 1998.

Olagnon, M., and G. A. Athanassoulis, eds., Rogue waves 2000, *Ifremer*, Actes de Colloques 32, 400 pp., 2001.

Onorato, M., A. Osborne, M. Serio, and S. Bertone, Freak Waves in Random Oceanic Sea States, *Phys. Rev. Lett., 86*, 5831, 2001a.

Onorato, M., A. Osborne, M. Serio and T. Damiani, Occurrence of Freak Waves from Envelope Equations in Random Ocean Simulations, *Rogue Waves 2000* (Olagnon and Athanassoulis, eds.), Ifremer, 2001b.

Osborne, A., M. Onorato, and M Serio, The nonlinear dynamics of rogue waves and holes in deep-water gravity wave trains, *Phys.*

Lett. A, 275, 386, 2000.

Pelinovsky, E., T. Talipova, and C. Kharif, Nonlinear dispersive mechanism of the freak wave formation in shallow water, *Physica D, 147*, 83, 2000.

Pelinovsky, E., C. Kharif, T. Talipova, and A. Slunyaev, Nonlinear wave focusing as a mechanism of the freak wave generation in the ocean, *Rogue Waves 2000* (Olagnon and Athanassoulis, eds.), Ifremer, 2001.

Trulsen, K. and K. Dysthe, A modified nonlinear Schrödinger equation for broader bandwidth gravity waves on deep water, *Wave Motion, 24*, 281-289, 1996.

Trulsen, K. and K. Dysthe, Frequency downshift in three-dimensional wave trains in a deep basin, *J. Fluid Mech., 352*, 359-373, 1997.

This preprint was prepared with AGU's LaTeX macros v4, with the extension package 'AGU++' by P. W. Daly, version 1.6a from 1999/05/21.